

BEAM DYNAMIC STUDY OF A COMPACT SUPERCONDUCTING SKELETON CYCLOTRON (SSC) FOR BNCT AND RADIOISOTOPE PRODUCTION

H. W. Koay[†], M. Fukuda, H. Kanda, T. Yorita
 Research Centre of Nuclear Physics, Osaka University, Japan

Abstract

This work presents a preliminary study on the beam dynamics of a compact superconducting skeleton cyclotron (SSC) for Boron Neutron Capture Therapy (BNCT) and radioisotope production. This work adopted an air-core structure to avoid any residual magnetisation from the hysteresis loop of an iron yoke. This leads to a higher reproducibility of magnetic field in a shorter time, which is very favourable for a hospital environment. The proposed design is a compact K-80 cyclotron with a small extraction radius of 40 cm for a 50 MeV H^+ and 40 MeV D^+ beam. It includes a series of combination of circular high-temperature superconducting (HTS) coil, acting as the main coil and trim coils, as well as 3 sector coils with a maximum spiral angle of 40° . In this work, the configuration of these coils is optimized to generate an isochronous field with adequate focusing force. On top of this, the corresponding equilibrium orbits for H^+ particle, and some important beam properties such as the phase excursion, betatron oscillation and beam focusing capability are also included in order to evaluate the feasibility of the generated magnetic field distribution.

INTRODUCTION

The implementation of accelerator-based BNCT (AB-BNCT) in a hospital environment has gained increasing attention nowadays due to promising clinical results shown in past study [1, 2, 3]. In order to realise this in a hospital, an AB-BNCT system should fulfil two important requirement: (a) compact and easy handling, (b) high beam intensity for a high neutron yield to shorten treatment time. Despite many superconducting cyclotrons engaging in medical application are available worldwide, most of them are huge and bulky, yet delivering beam of small current ($<100 \mu A$), as they focus solely on the production of radioisotopes used for medical diagnostic and therapeutic applications [4, 5]. Some works have been made to reduce the weight by adopting superconducting coils with iron core/sector. However, the saturation of iron cores limits the maximum magnetic field, which implicitly limits the compactness of the machine. In accordance with this, a design was proposed by Ueda et. al. using an air-core HTS sector coils with a split HTS main coils for heavy-ion therapy [6]. This design results in a lighter and a more compact machine that consumes less power, a higher reproducibility of magnetic field in a shorter time, as well as a simpler cooling system. Therefore, we wish to implement this idea in

the design of a high-current skeleton cyclotron for the implementation of a previously proposed BNCT system, which is the accelerator-based multi-port BNCT (AB-mBNCT) [7], as well as the production of medical radioisotopes. Figure 1 shows the schematic of this proposal. As a part of the study of SSC, this work will discuss about the primary configuration of the proposed SSC and the corresponding single-particle beam dynamic analysis.

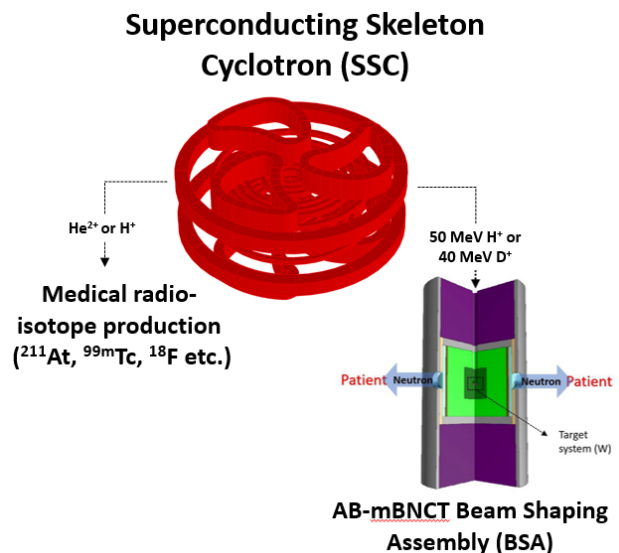


Figure 1: Schematic of the proposed SSC and its application for AB-mBNCT as well as radioisotope production.

MATERIAL AND METHOD

Design Specification

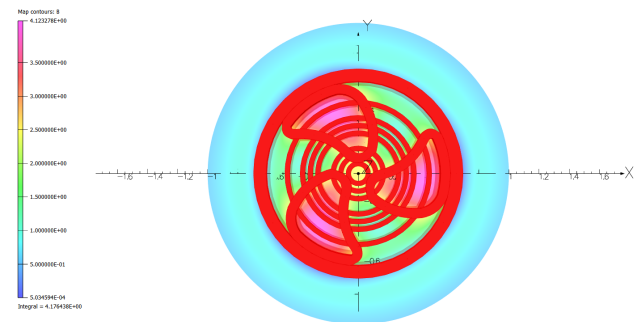


Figure 2: 2d magnetic distribution obtained at the median plane using the primary configuration of SSC proposed. This corresponds to the case of average B_z of 2.48 T.

[†] koay@rcnp.osaka-u.ac.jp

The proposed SSC is an air-core (i.e. meaning of “skeleton”) K-80 cyclotron with a small extraction radius of 40 cm for multiple-ion beams. The optimization of magnetic field distribution to achieve isochronism is provided by a series of combination of circular high-temperature superconducting coil (HTSC). These HTSC consists of 3 sector coils (SC) with a maximum spiral angle of 40°, 1 circular main coil (MC) of 60 cm radius and 7 small trim coils (TC) of radius varying from 5 cm to 45 cm. Some of the specification is shown in Table 1 below.

Table 1: The Specification of the Proposed SSC

Particle type	H ⁺	D ⁺	He ²⁺
Max energy (MeV)	50	40	40
Ave. magnetic field (T)	2.48	3.18	2.26
Revolution frequency (MHz)	37.4179	24.3969	17.3326
Harmonic mode	2 (push-push)		
Dee number/angle	2 / 90°		
Dee Voltage (kV)	80		
Sector number	3		
Max spiral angle	40°		
Extraction radius (cm)	~ 40		

Magnetic field distribution

The magnetic field distribution was calculated using the finite element magnetostatic (FEM) code TOSCA. The initial estimation of isochronous field is given by:

$$\langle B(\vec{r}) \rangle = \frac{B_0}{\sqrt{1-\beta(\vec{r})^2}} \quad (1)$$

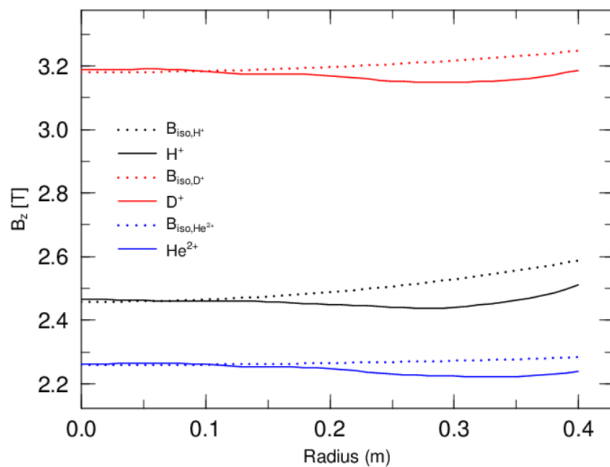


Figure 3: Average magnetic distribution for H⁺ (black), D⁺ (red) and He²⁺ (blue) ions up to 40 cm. Dotted lines show the analytical estimation of isochronous field using eqn. 1.

After that, we have used the OPAL (Object Oriented Parallel Accelerator Library) code to determine the orbital frequency ω_i of the closed orbit [8]. A better isochronous field $\langle B \rangle_{i+1}$ was obtained by re-scaling the input field $\langle B \rangle_i$ using the ω_i obtained from OPAL.

$$\langle B \rangle_{i+1} = \frac{\omega_{rv}}{\omega_i} \langle B \rangle_i \quad (2)$$

This process was repeated for several cycles until a satisfying phase lag was achieved. The radial dependence of average magnetic field and the corresponding flutter are shown in Fig. 3 and 4 respectively.

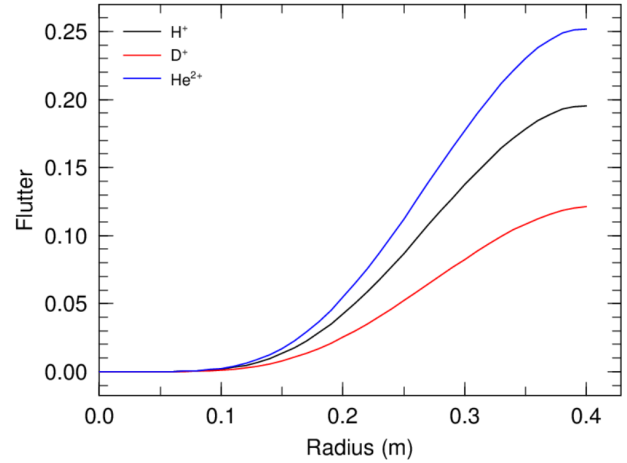


Figure 4: Flutter for H⁺, D⁺ and He²⁺ ions up to 40 cm.

RESULTS AND DISCUSSIONS

All the analysis of beam dynamics were performed by using OPAL-cycl mode of OPAL 2.0.1 developed by PSI [8]. Dee voltage of 0 kV and 80 kV were used for SEO and AEO analysis respectively. The gap size was assumed zero and the radial dependence of dee voltage was omitted. Only single H⁺ particle is involved in the following analysis, as this is the most important primary beam for AB-BNCT neutron source.

Static Equilibrium Orbit (SEO) Analysis

Betatron Oscillation The working tune diagram based on the designed field map is shown in Fig. 5. Although calculations show that the particle crosses a few third order resonances during the acceleration from 0.32 MeV up to 50 MeV, most of them are crossed rather quickly. Thus, the effect is not detrimental and it can be concluded that the designed magnetic field has a satisfying betatron oscillation except at around 40 MeV, where the particle fluctuates around the resonance region for a longer time. Further study to investigate the impact of those resonances on the beam stability is necessary in the coming future.

Phase Excursion The phase excursion computed using eqn. 3 is shown in Fig. 6. The harmonic number, h was assumed to be 2 and the initial phase ϕ_0 at $E_0 = 0.32$ MeV was taken to be 5°.

$$\sin \phi(E) = \sin \phi_o + \frac{2\pi h}{qV} \int_{E_o}^E \Omega(E) dE \quad (3)$$

From small fluctuation shown in Fig. 6, we can conclude that the magnetic field satisfies the isochronous condition well within $\pm 5^\circ$.

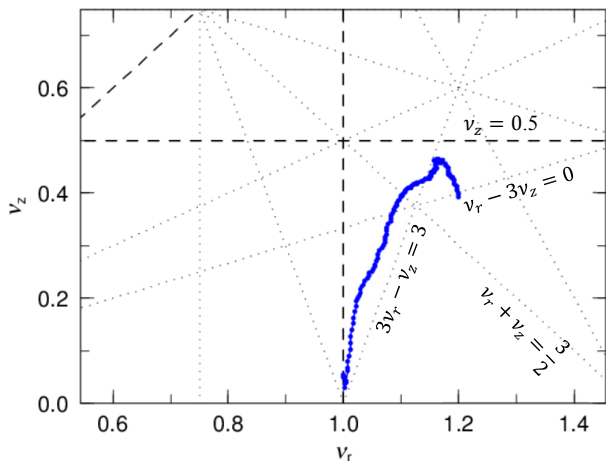


Figure 5: Betatron tune diagram of H⁺ ion for energy from 0.32 MeV up to 50 MeV.

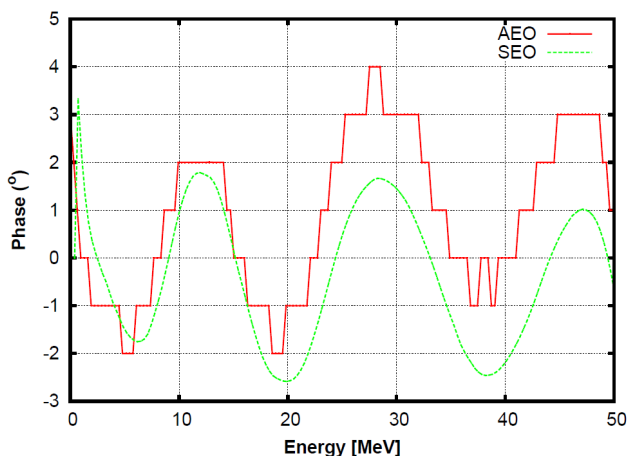


Figure 6: Phase excursion calculated from eqn. 3 for SEO (green) and the phase lag of RF obtained at the first gap of every turn for accelerated orbit (AEO).

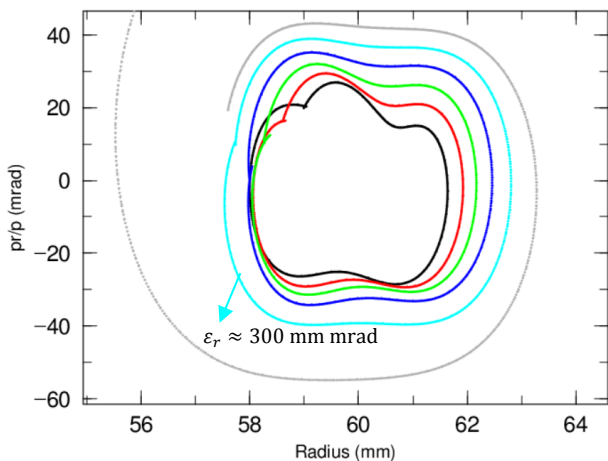


Figure 7: Radial phase diagram of 1 MeV beam obtained at zero azimuthal angle.

Stability Limit Owing to the existence of transverse focusing, there is a stability limit that a stray-away particle can remain in the beam oscillating steadily with the betatron frequency. However, beyond this limit, the particle will become unstable and it will never be able to return to the coasting orbit. Hence, it is very important to investigate this limit in order to determine the phase acceptance of the cyclotron. In accordance to this, this work also studied the radial phase diagram. Figure 7 shows the radial phase diagram evaluated at zero azimuthal angle for energy of 1 MeV. The stability limit is taken as the boundary of the biggest bounded area. From Fig. 7, the biggest bounded area is about 300 mm mrad. This corresponds to a satisfactory acceptance of 300 mm mrad at 1 MeV, which is sufficiently large to sustain the coasting beam.

Accelerated Equilibrium Orbit (AEO) Analysis

AEO Figure 8 shows one of the possible AEO from 20 keV up to a maximum energy of 50.2 MeV. It takes about 157 turns to reach the final energy and the final turn separation is about 2.3 mm. The phase excursion of AEO obtained at the first gap (20°) of every turn is shown in Fig. 5. Similar phase lag of $< 5^\circ$ shown by both AEO and SEO further confirms the isochronism of the designed magnetic field.

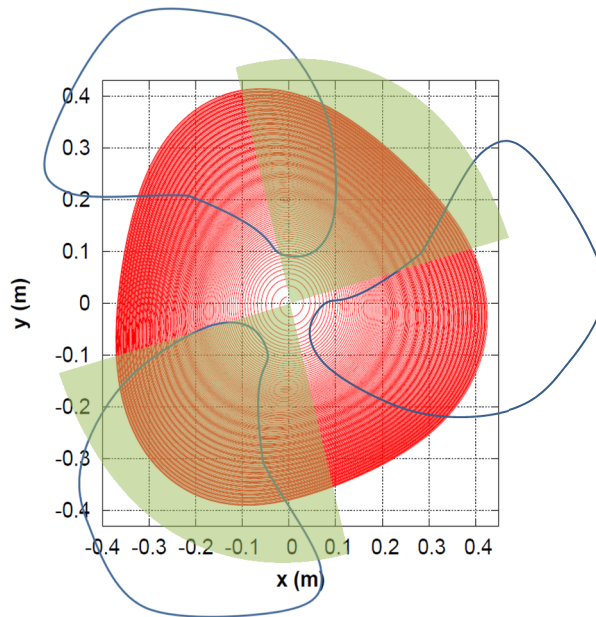


Figure 8: One of the possible AEO calculated in OPAL using 20 keV H⁺. The injection radius is 14.333 mm at 108° and the initial p_r is 0.002987 (~ 457 mrad).

Although Fig. 8 shows AEO without any overlap or crossover, the wavy structure indicates the existence of a precessional motion of the orbit center. This precessional motion is known as coherent oscillation. Coherent oscillation occurs due to an off-centered injection or any imperfection of the real magnetic field distribution. In ideal case, this oscillation can be compensated by introducing extra

harmonic coils (HC). However, a detailed study of the injection and extraction system remains as deciding factors that will change the current AEO significantly. Thus, the specification of HC shall remain as a part of the next study after fixing the injection and extraction system.

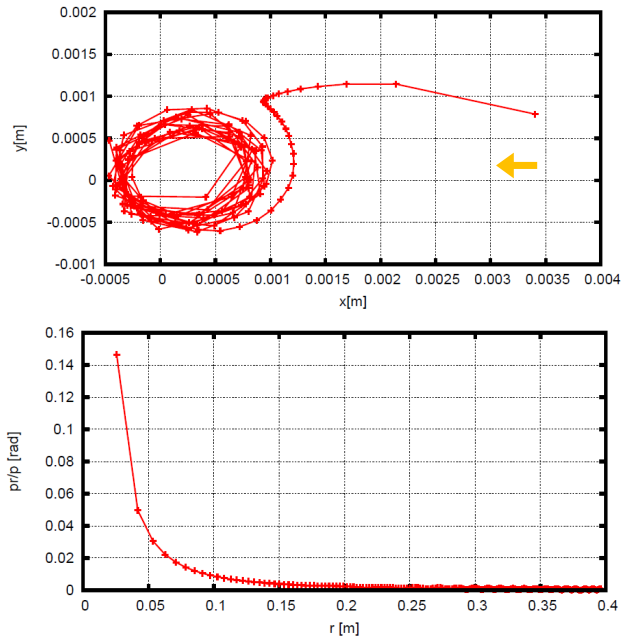


Figure 9: Off-centering motion of the orbit center from AEO in Fig. 8 expressed in term of Cartesian coordinate (top) and radial momentum (bottom).

Axial Focusing On top of coherent oscillation in radial direction, it is also important to determine the axial oscillation in AEO. Figure 9 shows off-centered axial motion with respect to the reference particle (purple line) for several initial condition bounded by an emittance of 10π mrad.

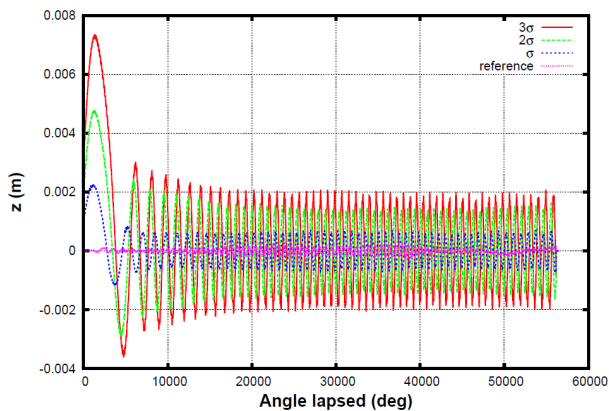


Figure 10: Axial motion of particle assuming an initial $[z$ (mm), p_z (mrad)] of $[3, 10]$ (red); $[2, 6.67]$ (green); $[1, 3.3]$ (blue) and $[0, 0]$ (purple).

Figure 10 shows that the red line, which has the largest divergence, increases significantly at the first few turns. Nevertheless, this large amplitude is immediately reduced

and confined to less than 3 mm after the 13th turn. Generally, the maximum amplitude is less than 1 cm. This is smaller than the planned vertical aperture of the dee cavity of 2~3 cm. Hence, we can conclude that at current stage, the axial focusing provided by the designed field is sufficient. However, this is only the case for single particle motion. The beam envelope will increase significantly when the space charge effect is taken into account in bunch calculation. This shall also remain as a part of our next study.

CONCLUSION

In conclusion, the satisfactory performance shown by the single-particle beam dynamic analysis confirms the feasibility of the proposed SSC. The SEO shows a satisfactory isochronism of magnetic field distribution and betatron oscillation, while the AEO analysis confirms the stability of the coasting orbit during acceleration using the proposed SSC. On top of this, owing to the air-core structure and small extraction radius, the proposed SSC is expected to be compact and lighter than most of the currently available medical cyclotron. This fulfils our first requirement for the installation in a hospital environment. As for the second requirement, i.e. to produce a high intensity beam, there are some other aspects which require further investigation. These include the injection and extraction system, the installation of HC, as well as the single and multi-bunch calculations which take into account of the space charge effect.

REFERENCES

- [1] S. Kawabata, M. Shin-ichi, K. Toshihiko, K. Yokoyama, A. Doi, K. Iida, S. Miyata, N. Nonoguchi, H. Michiue, M. Takahashi, T. Inomata, Y. Imahori, M. Kirihata, Y. Sakurai, A. Maruhashi, H. Kumada and K. Ono, "Boron Neutron Capture Therapy for Newly Diagnosed Glioblastoma," *Journal of Radiation Research*, vol. 50, no. 1, pp. 51-60, 2009.
- [2] T.-L. Lan, F.-I. Chou, W.-S. Huang, K.-H. Lin, Y.-Y. Lee, P.-S. Pan, Y.-C. Kuo, S.-M. Hsu, F.-C. Chang, M.-L. Liang, J.-C. Lee, S.-C. Lin, Y.-M. Liu, Y. Chao and Y.-W. Chen, "Overt tumor regression after salvage boron neutron capture therapy (BNCT) for a recurrent glioblastoma patient," *Therapeutic Radiology and Oncology*, vol. 2, no. 0, 2018.
- [3] I. Kato, K. Ono, Y. Sakurai, M. Ohmae, A. Maruhashi, Y. Imahori, M. Kirihata, M. Nakazawa and Y. Yura, "Effectiveness of BNCT for recurrent head and neck malignancies," *Applied Radiation and Isotopes*, vol. 61, no. 5, pp. 1069-1073, 2004.
- [4] A. Geisler, J. Hottenbacher, H.-U. Klein, D. Krischel, H. Röcken and C. Baumgarten, "Commissioning of the ACCEL 250 MEV Proton Cyclotron," in *Cyclotrons and Their Applications, Eighteenth International Conference*, 2007.
- [5] V. Smirnov, S. Vorozhtsov and J. Vincent, "Design study of an ultra-compact superconducting cyclotron for isotope production," *Nuclear Instruments and Methods in Physics Research Section A: Accelerators, Spectrometers, Detectors and Associated Equipment*, vol. 763, pp. 6-12, 2014.
- [6] H. Ueda, M. Fukuda, K. Hatanaka, T. Wang, X. Wang, A. Ishiyama, S. Noguchi, S. Nagaya, N. Kashima and N. Miyahara, "Conceptual Design of Next Generation HTS Cyclotron," *IEEE Transactions on Applied Superconductivity*, vol. 23, no. 3, 2013.
- [7] H. W. Koay, M. Fukuda, H. Toki, R. Seki, H. Kanda and T. Yorita, "Feasibility study of compact accelerator-based

neutron generator for multi-port BNCT system,” *Nuclear Instruments and Methods in Physics Research Section A: Accelerators, Spectrometers, Detectors and Associated Equipment*, vol. 899, pp. 65-72, 2018.

- [8] A. Adelman, P. Calvo, M. Frey, A. Gsell, U. Locans, C. Metzger-Kraus, N. Neveu, C. Rogers, S. Russell, S. Sheehy, J. Snuverink and D. Winklehner, “OPAL a Versatile Tool for Charged Particle Accelerator Simulations,” *Journal of Computational Physics*, vol. arXiv preprint arXiv:1905.06654, 2019.